Arabian Journal of Chemistry (2022) 15, 104160

King Saud University

Arabian Journal of Chemistry

www.ksu.edu.sa
www.sciencedirect.com

ORIGINAL ARTICLE

Topological properties of reverse-degree-based indices for sodalite materials network

Ali N.A. Koam [a], Moin A. Ansari [a,*], Azeem Haider [a], Ali Ahmad [b], Muhammad Azeem [c]

[a] Department of Mathametics, College of Science, Jazan University, Jazan, Saudi Arabia
[b] College of Compiuter Science, Jazan University, Jazan, Saudi Arabia
[c] Department of Mathematics, Riphah Institute of Computing and Applied Sciences, Riphah International University Lahore, Pakistan

Received 1 March 2022; accepted 27 July 2022
Available online 2 August 2022

KEYWORDS

Sodalite materials network;
Topological indices;
Reverse degree;
Natural zeolites

Abstract Natural zeolites are frequently referred to as macromolecular sieves. Because of relatively inexpensive cost of installation, zeolites networks are highly trendy chemical networks. Amongst the most researched types of zeolite networks is the sodalite network. It contributes to the elimination of greenhouse gases. To investigate the above widely tested, we employ an authentic mathematical tool known as topological descriptors or index, which displays some physical and chemical properties numerically. To fully comprehend the structure, we compare different legitimate properties via topological indices, concluding in the form of figurative comparisons. In particularly, we measure some reverse degree-based indices for the sodalite materials network and put some light on the behavior of this network, in the form of topological descriptors and numerically designed equation of such network. This research is novel in terms of no one studied reverse-degree-based topological indices for this chosen structure.

1. Introduction

Macromolecular sieves, typically described as natural zeolites, are being examined and investigated deeper (Neeraj et al., 2002; Karagiaridi et al., 2012; Eddaoudi et al., 2002). Zeolite's design atomic capture enables it noteworthy and broadly useful. Natural zeolites are helpful in high volume mineral usage because of their cheaper cost, according to Catlow (1992). Zeolites are classified into distinct classes based on their complexity and size. Stilbite, tschernichite, modernite, faujasite, sodalite, chabazite, for example, the one most beneficial in industrial purposes are molecular sieves, or natural zeolites, according to Dyer (1988). From those of the zeolite structures mentioned previously, synthesised compounds and mineral crystal structures with sodalite frameworks are the most extensively investigated substances (Jaeger, 1929; Pauling, 1930). The authors of Prabhu et al. (2020),

* Corresponding author at: Department of Mathematics, College of Science, Jazan University, Jazan, Saudi Arabia.
E-mail addresses: akoum@jazanu.edu.sa (A.N.A. Koam), maansari@jazanu.edu.sa (M.A. Ansari), aahaider@jazanu.edu.sa (A. Haider), ahmadsms@gmail.com (A. Ahmad), azeemali7009@gmail.com (M. Azeem).
Peer review under responsibility of King Saud University.

ELSEVIER Production and hosting by Elsevier

https://doi.org/10.1016/j.arabjc.2022.104160
1878-5352

Torrens and Castellano (2006), Torrens and Castellano (2019), discussed for certain chemical and physical characteristics of zeolite type structures particularly sodalite when it comes to the form of topological indices.

Sodalites already have best thermodynamic consistency and are regarded as one of the highest rated structures across all zeolites (Barth, 1932; Hassan and Grundy, 1984). Because of their crystallographic positions, sodalites are also significant, according to Taylor (1967). The unit cell of the sodalite structure is comprised of two cages. Each cage's fundamental structure consists of six and four membered rings. Two parallel cages also share these rings. For capture molecules, cavities in sodalite are built by using a custom-made mixture, Arockiaraj et al. (2021). Tap molecules, such as water and CO_2, already have capacity to desorb and adsorb molecules without causing damage to the crystal structures. As a result, Arockiaraj et al. (2021) for the use of zeolites in the removal of greenhouse gases and water. See Jiri et al. (2007), Keeffe (1991), for more research on zeolites, sodalite, and their practical uses.

Topological descriptor is a mechanism that, especially quantitative form, illustrates the physical, chemical and biological properties of a provided chemical graph in domain in a comprehensive way. The following definitions include few more topological indices that are both fascinating and usually praised, as well as their introducers. According to Ajmal et al. (2016), the researchers investigated polyhex and prism structures in terms of various indices. In Munir et al. (2016), titania nanotubes are analysed in terms of various topological descriptors. Authors of Munir et al. (2016), investigated the structure of dendrimers of nanostar and structure of nanotubes provided by polyhex. We refer to Nadeem et al. (2021), Nadeem et al. (2021), for a few intriguing discussion of chemical structures and their graphical features and diverse forms. There are several methods and different kinds of computing topological indices for different structures, such as in Shabbir et al. (2020), measured the edge-degree-based topological indices, Nadeem et al. (2021), Hong et al. (2020), metal organic structure is found in terms of topological indices, graphs resulted in the line graph operation and their results on the topological descriptors are available in Nadeem et al. (2016), Nadeem et al. (2019). Relative topics of applied graph theory in chemistry or using the chemical structures are found in Koam et al. (2022), Koam et al. (2022), Hameed et al. (2022), Alshehri et al. (2022), Koam et al. (2022), Azeem et al. (2022). Certain new research which are available at Liu et al. (2020), and also for further information on latest networks and their topological descriptors.

2. Preliminaries

To determine these primary outcomes, we must first specify certain fundamentals, let χ be a corresponded graph of a network having the bonds E, and atoms labels as V. Where the notion $|V|$ symbolized as the total numbers of nodes or atoms and $|E|$ contributed as edge or bonds count. Let the notion d_θ contributed as degree of a vertex θ and defined as the count of edges attached to this vertex. The researcher from Kulli (2018), introduced another concept labeled as reverse-degree and symbolized as $\mathfrak{r}_\theta$. This newly developed notion is mathematically stated as $\mathfrak{r}_\theta = 1 + \Delta - d_\theta$, in which the parameter Δ denotes the utmost degree of a vertex of a network. A notion $\mathbf{E}_{\mathfrak{r}_\theta,\mathfrak{r}_\vartheta}$ labeled as an edge partition of a network designed on the concept of reverse-degree of end vertices of an edge $\theta\vartheta \in E$. Similarly, the notion $|\mathbf{E}_{\mathfrak{r}_\theta,\mathfrak{r}_\vartheta}|$ contributed as its cardinality.

A general topological descriptor $\mathscr{I}(\chi)$, based on the reverse-degree of a vertex stated as Mufti et al. (2022):

$$\mathscr{I}(\chi) = \sum_{\theta\vartheta \in E(\chi)} \Pi(\mathfrak{r}_\theta, \mathfrak{r}_\vartheta). \tag{1}$$

Given by Zhao et al. (2021), Wang et al. (2020)

$$\begin{aligned} &\text{Let } \Pi(\mathfrak{r}_\theta,\mathfrak{r}_\vartheta) = (\mathfrak{r}_\theta \times \mathfrak{r}_\vartheta)^\alpha. \\ &\text{Then } \mathscr{I}(\chi) \text{ symbolises the general reverse Randic}' \\ &\text{descriptor } (\mathfrak{r}\mathbb{R}_\alpha(\chi)) \text{ for } \alpha = \tfrac{1}{2}, -\tfrac{1}{2}, 1, -1. \text{If } \alpha = 1, \\ &\text{then it is known as the second reverse Zagreb descriptor} \\ &(\mathfrak{r}\mathbb{M}_2(\chi)). \end{aligned} \tag{2}$$

Found in Koam et al. (2021)

$$\begin{aligned} &\text{Let } \Pi(\mathfrak{r}_\theta,\mathfrak{r}_\vartheta) = \sqrt{\frac{\mathfrak{r}_\theta + \mathfrak{r}_\vartheta - 2}{\mathfrak{r}_\theta \times \mathfrak{r}_\vartheta}}. \\ &\text{Then } \mathscr{I}(\chi) \text{ symbolises the reverse atom-bond} \\ &\text{connectivity descriptor } (\mathfrak{r}\mathbb{ABC}(\chi)). \end{aligned} \tag{3}$$

Described in Jayanna and Swamy (2021), Gao et al. (2018)

$$\begin{aligned} &\text{Let } \Pi(\mathfrak{r}_\theta,\mathfrak{r}_\vartheta) = \frac{2\sqrt{\mathfrak{r}_\theta \times \mathfrak{r}_\vartheta}}{\mathfrak{r}_\theta + \mathfrak{r}_\vartheta}. \text{ Then } \mathscr{I}(\chi) \\ &\quad \text{symbolises the reverse geometric}- \\ &\text{arithmetic descriptor } (\mathfrak{r}\mathbb{GA}(\chi)). \end{aligned} \tag{4}$$

$$\begin{aligned} &\text{Let } \Pi(\mathfrak{r}_\theta,\mathfrak{r}_\vartheta) = (\mathfrak{r}_\theta + \mathfrak{r}_\vartheta). \\ &\quad \text{Then } \mathscr{I}(\chi) \text{ symbolises the first reverse Zagreb} \\ &\text{descriptor } (\mathfrak{r}\mathbb{M}_1(\chi)). \end{aligned} \tag{5}$$

Found in Wang et al. (2020), Poojary et al. (2022)

$$\begin{aligned} &\text{Let } \Pi(\mathfrak{r}_\theta,\mathfrak{r}_\vartheta) = (\mathfrak{r}_\theta + \mathfrak{r}_\vartheta)^2. \text{ Then } \mathscr{I}(\chi) \\ &\quad \text{symbolises the reverse hyper} \\ &\text{Zagreb descriptor } (\mathfrak{r}\mathbb{HM}(\chi)). \end{aligned} \tag{6}$$

$$\begin{aligned} &\text{Let } \Pi(\mathfrak{r}_\theta,\mathfrak{r}_\vartheta) = \left((\mathfrak{r}_\theta)^2 + (\mathfrak{r}_\vartheta)^2\right). \\ &\quad \text{Then } \mathscr{I}(\chi) \text{ symbolises the reverse forgotten} \\ &\text{descriptor } (\mathfrak{r}\mathbb{F}(\chi)). \end{aligned} \tag{7}$$

Formulated in Wang et al. (2020)

$$\begin{aligned} &\text{Let } \Pi(\mathfrak{r}_\theta,\mathfrak{r}_\vartheta) = (\mathfrak{r}_\theta + \mathfrak{r}_\vartheta)^\alpha(\mathfrak{r}_\theta \times \mathfrak{r}_\vartheta)^\beta. \text{ Then } \mathscr{I}(\chi) \text{ symbolises} \\ &\quad \text{the first reverse redefined descriptor } (\mathfrak{r}\mathbb{R}\mathbb{e}\mathbb{Z}_1(\chi)) \\ &\qquad \text{for } \alpha = 1, \beta = -1; \\ &\quad \text{the second reverse redefined descriptor } (\mathfrak{r}\mathbb{R}\mathbb{e}\mathbb{Z}_2(\chi)) \\ &\qquad \text{for } \alpha = -1, \beta = 1. \\ &\quad \text{the third reverse redefined descriptor } (\mathfrak{r}\mathbb{R}\mathbb{e}\mathbb{Z}_3(\chi)) \\ &\qquad \text{for } \alpha = 1, \beta = 1. \end{aligned} \tag{8}$$

Furthermore, the flowchart of the methodology defined above is shown in the Fig. 1.

3. Structure of sodalite materials

The three-dimensional sodalite network $\chi_{l,w,h}$ is shown in Fig. 2. It has a total of $4(lw + lh + wh) + 12lwh$ vertices as well as the total number of edges. Where l, w, h are parameters to show the copies of structure into vertically (length), inside the page (width) and horizontally (height), respectively. It has two types of atoms and three types of bonds, as illustrated in the Fig. 2, and these are beneficial to the key outcomes. The Fig. 2 is investigated in detail given by Arockiaraj et al. (2021), as well as to investigate several beneficial structures linked to

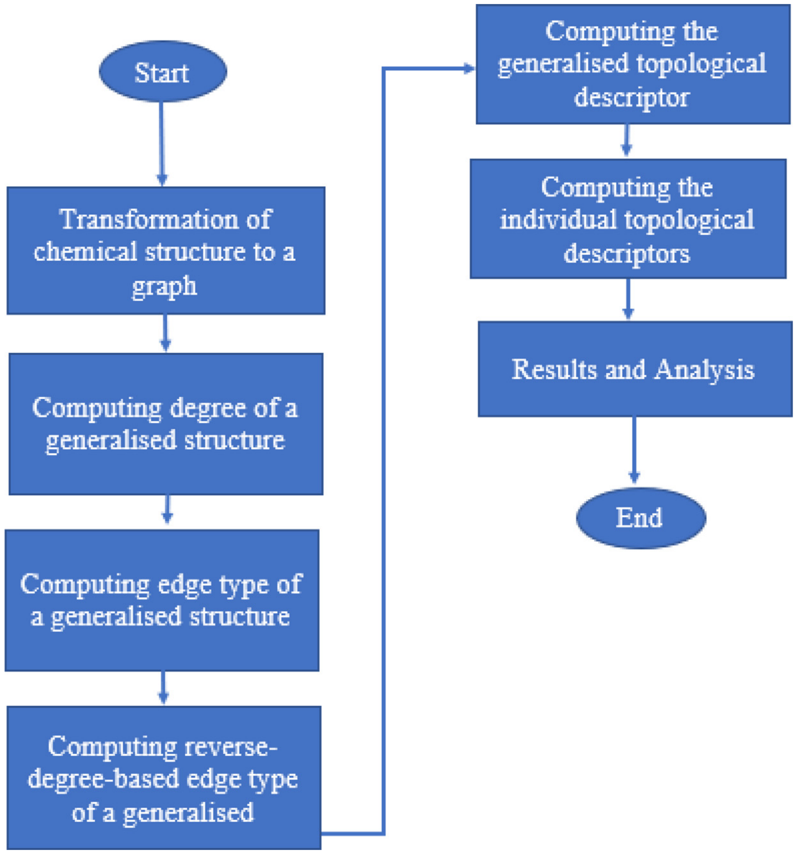

Fig. 1 Flowchart to measure a reverse-degree-based topological descriptor.

zeolites and sodalite. Very first outcome is the sodalite network's primary and general reverse-degree-based topological indices $\chi_{l,w,h}$.

4. Main results

Throughout this study, we looked at the sodalite three-dimensional structure, that is a component of the zeolite network, in terms of the various reverse-degree-based topological indices mentioned previously. Furthermore, we describe the structure further explicitly by using various numerical instances and conducting a comparison examination of computed M-polynomials, and we finish in the diagrammatical visualizations of generated mathematical formulation. For latest results on topological indices see Ahmad (2020), Zhang et al. (2020), Zahra et al. (2020), Randic (1975), Siddiqui et al. (2016), Aslam et al. (2017), Javaid et al. (2021), Liu et al. (2020), Refaee and Ahmad (2021).

Lemma 4.1. *Let $\chi_{l,w,h}$ be a sodalite network. Then*

$\mathscr{I}_1(\chi_{l,w,h}) = 24lwh(\Pi(1,1)) + 4(lw+wh+lh)(-3\Pi(1,1)+2\Pi(1,2)+2\Pi(2,2))+4(l+w+h)(\Pi(1,1)-2\Pi(1,2)+\Pi(2,2))$.

Proof. The graph $\chi_{l,w,h}$ contains $24lwh+4(lw+wh+lh)$ edges and maximum degree in $\chi_{l,w,h}$ graph is 4. The graph of $\chi_{l,w,h}$ contained two forms of reverse-degree vertices which are 1 and 2. Let us partitioned the atoms of $\chi_{l,w,h}$ based on its reverse-degrees as:

$$\mathbf{E}_{1,1} = \{\theta\vartheta \in E(\chi_{l,w,h}) : \mathfrak{r}_\theta = 1, \mathfrak{r}_\vartheta = 1\} \tag{9}$$
$$\mathbf{E}_{1,2} = \{\theta\vartheta \in E(\chi_{l,w,h}) : \mathfrak{r}_\theta = 1, \mathfrak{r}_\vartheta = 2\} \tag{10}$$
$$\mathbf{E}_{2,2} = \{\theta\vartheta \in E(\chi_{l,w,h}) : \mathfrak{r}_\theta = 2, \mathfrak{r}_\vartheta = 2\} \tag{11}$$

Note that $E(\chi_{l,w,h}) = \mathbf{E}_{1,1} \cup \mathbf{E}_{1,2} \cup \mathbf{E}_{2,2}$ and $|\mathbf{E}_{1,1}| = 24lwh - 12(lw+wh+lh)+4(l+w+h), |\mathbf{E}_{1,2}| = 8(lw+wh+lh-l-w-h)$, $|\mathbf{E}_{2,2}| = 8(lw+wh+lh)+4(l+w+h)$. Hence,

$$\begin{aligned}
\mathscr{I}_1(\chi_{l,w,h}) &= \sum_{\theta\vartheta\in E(\chi_{l,w,h})} \Pi(\mathfrak{r}_\theta, \mathfrak{r}_\vartheta) \\
&= \sum_{\theta\vartheta\in \mathbf{E}_{1,1}} \Pi(1,1) + \sum_{\theta\vartheta\in \mathbf{E}_{1,2}} \Pi(1,2) + \sum_{\theta\vartheta\in \mathbf{E}_{2,2}} \Pi(2,2) \\
&= (24lwh - 12(lw+wh+lh)+4(l+w+h))\Pi(1,1) \\
&\quad +8(lw+wh+lh-l-w-h)\Pi(1,2) \\
&\quad +(8(lw+wh+lh)+4(l+w+h))\Pi(2,2).
\end{aligned}$$

After simplification, we get

$\mathscr{I}_1(\chi_{l,w,h}) = 24lwh(\Pi(1,1)) + 4(lw+wh+lh)(-3\Pi(1,1)+2\Pi(1,2)+2\Pi(2,2)) + 4(l+w+h)(\Pi(1,1)-2\Pi(1,2)+\Pi(2,2))$. □

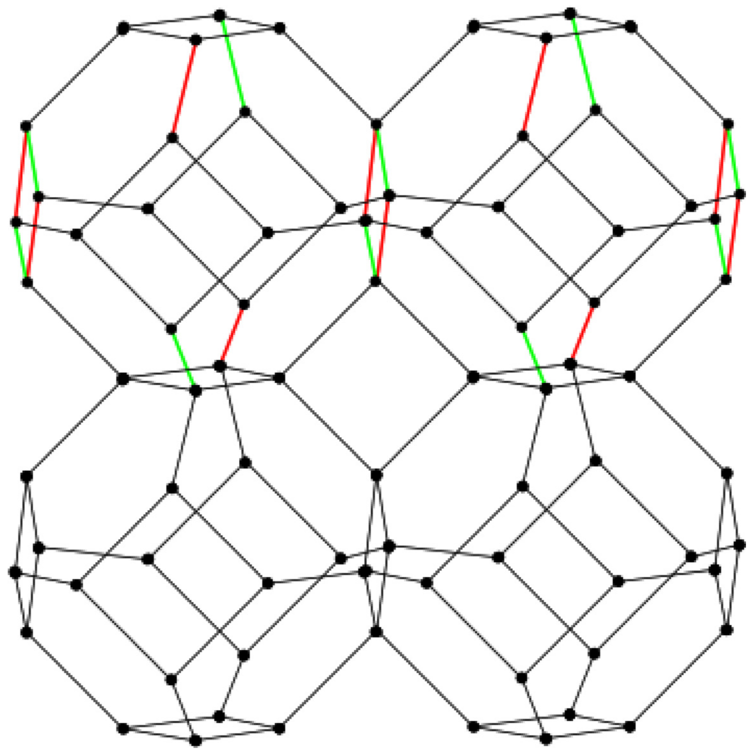

Fig. 2 $\chi_{2,2,1}$ or Sodalite network.

Theorem 4.2. *The general reverse Randić index of $\chi_{l,w,h}$ is equal to*

$$\mathrm{r}\mathbb{R}_\alpha(\chi_{l,w,h}) = \begin{cases} 24lwh + 36(lw+wh+lh) + 4(l+w+h), & \text{for } \alpha = 1 \\ 24lwh + 4(lw+wh+lh)\big(1+2\sqrt{2}\big) \\ \quad +4(l+w+h)\big(1-2\sqrt{2}\big), & \text{for } \alpha = \frac{1}{2} \\ 24lwh + 4(lw+wh+lh)\big(-2+\sqrt{2}\big) \\ \quad +4(l+w+h)\big(\frac{3}{2}-\sqrt{2}\big), & \text{for } \alpha = \frac{-1}{2} \\ 24lwh - 6(lw+wh+lh) + 2(l+w+h), & \text{for } \alpha = -1. \end{cases}$$

Proof. For $\mathrm{r}\mathbb{R}_\alpha(\chi_{l,w,h})$ that is a general reverse Randić index of $\chi_{l,w,h}$, from Eq. (2), we will get $\Pi(\mathrm{r}_\theta, \mathrm{r}_\vartheta) = (\mathrm{r}_\theta \times \mathrm{r}_\vartheta)^\alpha$, therefore $\Pi(1,1) = 1, \Pi(1,2) = 2^\alpha$ and $\Pi(2,2) = 2^{2\alpha}$. Thus by Lemma 4.1,

$$\mathrm{r}\mathbb{R}_\alpha(\chi_{l,w,h})) = 24lwh + 4(lw+wh+lh)\big(-3+2^{\alpha+1}+2^{2\alpha+1}\big) + 4(l+w+h)\big(1-2^{\alpha+1}+2^{2\alpha}\big).$$

Put $\alpha = 1$, we will get

$$\mathrm{r}\mathbb{R}_1(\chi_{l,w,h})) = 24lwh + 36(lw+wh+lh) + 4(l+w+h).$$

Put $\alpha = \frac{1}{2}$, we will get

$$\mathrm{r}\mathbb{R}_{\frac{1}{2}}(\chi_{l,w,h})) = 24lwh + 4(lw+wh+lh)\Big(1+2\sqrt{2}\Big) + 4(l+w+h)\Big(1-2\sqrt{2}\Big).$$

Put $\alpha = \frac{-1}{2}$, we will get

$$\mathrm{r}\mathbb{R}_{\frac{-1}{2}}(\chi_{l,w,h})) = 24lwh + 4(lw+wh+lh)\Big(-2+\sqrt{2}\Big) + 4(l+w+h)\left(\frac{3}{2}-\sqrt{2}\right).$$

Put $\alpha = -1$, we will get

$$\mathrm{r}\mathbb{R}_{-1}(\chi_{l,w,h})) = 24lwh - 6(lw+wh+lh) + 2(l+w+h).$$

□

Theorem 4.3. *Let $\chi_{l,w,h}$ be a sodalite materials networks. Then the reverse atom-bond connectivity index:*

$$\mathrm{r}\mathbb{ABC}(\chi_{l,w,h}) = 8\sqrt{2}(lw+wh+lh) - 2\sqrt{2}(l+w+h)$$

the reverse geometric-arithmetic index:

$$\mathrm{r}\mathbb{GA}(\chi_{l,w,h}) = 24lwh + 4\left(-1+\frac{4\sqrt{2}}{3}\right)(lw+wh+lh) + 4(l+w+h)\left(2-\frac{4\sqrt{2}}{3}\right)$$

the first reverse Zagreb index:

$$\mathrm{r}\mathbb{M}_1(\chi_{l,w,h})) = 48lwh + 32(lw+wh+lh)$$

the reverse hyper Zagreb index:

$$\mathrm{r}\mathbb{HM}(\chi_{l,w,h}) = 94lwh + 152(lw+wh+lh) + 8(l+w+h)$$

the reverse forgotten index:

$$\mathrm{r}\mathbb{F}(\chi_{l,w,h}) = 48lwh + 80(lw+wh+lh).$$

Proof. For $r\mathbb{ABC}(\chi_{l,w,h})$ that is a reverse atom-bond connectivity index of $\chi_{l,w,h}$, from Eq. (3), we will get $\Pi(\mathfrak{r}_\theta,\mathfrak{r}_\vartheta)=\sqrt{\frac{\mathfrak{r}_\theta+\mathfrak{r}_\vartheta-2}{\mathfrak{r}_\theta\times\mathfrak{r}_\vartheta}}$, therefore $\Pi(1,1)=0$ and $\Pi(1,2)=\Pi(2,2)=\frac{1}{\sqrt{2}}$. Thus by Lemma 4.1 and after simplification,

$$r\mathbb{ABC}(\chi_{l,w,h})=8\sqrt{2}(lw+wh+lh)-2\sqrt{2}(l+w+h).$$

For $r\mathbb{GA}(\chi_{l,w,h})$ that is a reverse geometric-arithmetic index of $\chi_{l,w,h}$, from Eq. (4), we will get $\Pi(\mathfrak{r}_\theta,\mathfrak{r}_\vartheta)=\frac{2\sqrt{\mathfrak{r}_\theta\times\mathfrak{r}_\vartheta}}{\mathfrak{r}_\theta+\mathfrak{r}_\vartheta}$, therefore $\Pi(1,1)=1,\Pi(1,2)=\frac{2\sqrt{2}}{3}$ and $\Pi(2,2)=1$. Thus by Lemma 4.1 and after simplification,

$$r\mathbb{GA}(\chi_{l,w,h})=24lwh+4\left(-1+\frac{4\sqrt{2}}{3}\right)(lw+wh+lh)+4(l+w+h)\left(2-\frac{4\sqrt{2}}{3}\right).$$

For $r\mathbb{M}_1(\chi_{l,w,h})$ that is a first reverse Zagreb index of $\chi_{l,w,h}$, from Eq. (5), we will get $\Pi(\mathfrak{r}_\theta,\mathfrak{r}_\vartheta)=(\mathfrak{r}_\theta+\mathfrak{r}_\vartheta)$, therefore $\Pi(1,1)=2,\Pi(1,2)=3$ and $\Pi(2,2)=4$. Thus by Lemma 4.1 and after simplification,

$$r\mathbb{M}_1(\chi_{l,w,h}))=48lwh+32(lw+wh+lh).$$

For $r\mathbb{HM}(\chi_{l,w,h})$ that is a first reverse hyper Zagreb index of $\chi_{l,w,h}$, from Eq. (6), we will get $\Pi(\mathfrak{r}_\theta,\mathfrak{r}_\vartheta)=(\mathfrak{r}_\theta+\mathfrak{r}_\vartheta)^2$, therefore $\Pi(1,1)=4,\Pi(1,2)=9$ and $\Pi(2,2)=16$. Thus by Lemma 4.1 and after simplification,

$$r\mathbb{HM}(\chi_{l,w,h})=94lwh+152(lw+wh+lh)+8(l+w+h).$$

For $r\mathbb{F}(\chi_{l,w,h})$ that is a reverse forgotten index of $\chi_{l,w,h}$, from Eq. (7), we will get $\Pi(\mathfrak{r}_\theta,\mathfrak{r}_\vartheta)=\left((\mathfrak{r}_\theta)^2+(\mathfrak{r}_\vartheta)^2\right)$, therefore $\Pi(1,1)=2,\Pi(1,2)=5$ and $\Pi(2,2)=8$. Thus by Lemma 4.1 and after simplification,

$$r\mathbb{F}(\chi_{l,w,h})=48lwh+80(lw+wh+lh).$$

□

Theorem 4.4. *Let $\chi_{l,w,h}$ be a sodalite materials networks. Then the first reverse redefined index:*

$$r\mathbb{ReZ}_1(\chi_{l,w,h})=48\ lwh-4(lw+wh+lh)$$

the second reverse redefined index:

$$r\mathbb{ReZ}_2(\chi_{l,w,h})=12\ lwh+\frac{22}{3}(lw+wh+lh)+\frac{2}{3}(l+w+h)$$

the third reverse redefined index:

$$r\mathbb{ReZ}_3(\chi_{l,w,h})=48\ lwh+152(lw+wh+lh)+24(l+w+h).$$

Proof. For $r\mathbb{ReZ}_1(\chi_{l,w,h})$ that is a first reverse redefined index of $\chi_{l,w,h}$, from Eq. (8), we will get $\Pi(\mathfrak{r}_\theta,\mathfrak{r}_\vartheta)=(\mathfrak{r}_\theta+\mathfrak{r}_\vartheta)^1(\mathfrak{r}_\theta\times\mathfrak{r}_\vartheta)^{-1}$, therefore $\Pi(1,1)=2,\Pi(1,2)=\frac{3}{2}$ and $\Pi(2,2)=1$. Thus by Lemma 4.1 and after simplification,

$$r\mathbb{ReZ}_1(\chi_{l,w,h})=48\ lwh-4(lw+wh+lh)$$

For $r\mathbb{ReZ}_2(\chi_{l,w,h})$ that is a second reverse redefined index of $\chi_{l,w,h}$, from Eq. (8), we will get $\Pi(\mathfrak{r}_\theta,\mathfrak{r}_\vartheta)=(\mathfrak{r}_\theta+\mathfrak{r}_\vartheta)^{-1}(\mathfrak{r}_\theta\times\mathfrak{r}_\vartheta)^1$, therefore $\Pi(1,1)=\frac{1}{2},\Pi(1,2)=\frac{2}{3}$ and $\Pi(2,2)=1$. Thus by Lemma 4.1 and after simplification,

$$r\mathbb{ReZ}_2(\chi_{l,w,h})=12\ lwh+\frac{22}{3}(lw+wh+lh)+\frac{2}{3}(l+w+h)$$

For $r\mathbb{ReZ}_3(\chi_{l,w,h})$ that is a third reverse redefined index of $\chi_{l,w,h}$, from Eq. (8), we will get $\Pi(\mathfrak{r}_\theta,\mathfrak{r}_\vartheta)=(\mathfrak{r}_\theta+\mathfrak{r}_\vartheta)(\mathfrak{r}_\theta\times\mathfrak{r}_\vartheta)$, therefore $\Pi(1,1)=2,\Pi(1,2)=6$ and $\Pi(2,2)=16$. Thus by Lemma 4.1 and after simplification,

$$r\mathbb{ReZ}_3(\chi_{l,w,h})=48\ lwh+152(lw+wh+lh)+24(l+w+h).$$

□

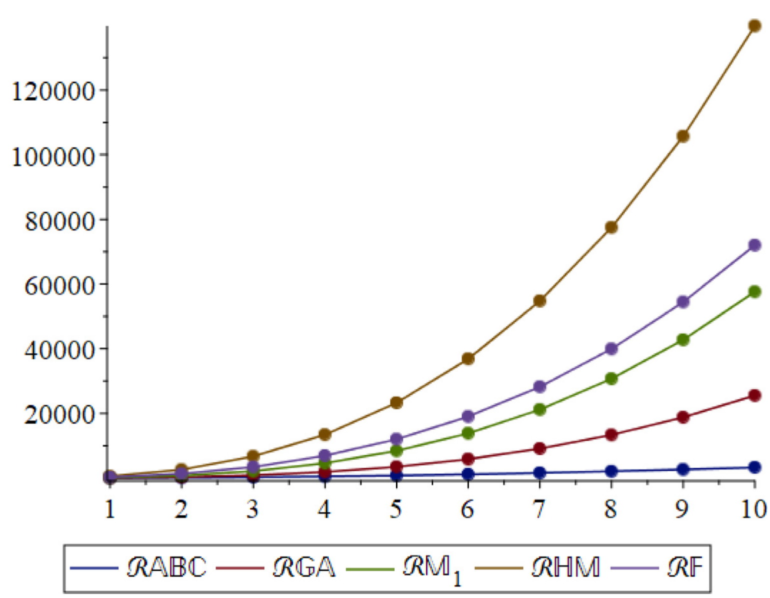

Fig. 3 Graphical analysis of $r\mathbb{ABC}, r\mathbb{GA}, r\mathbb{M}_1, r\mathbb{HM}$ and $r\mathbb{F}$ for sodalite materials networks, x-axis shows the numeral values of parameters l, w, h and y-axis shows the resulted values of descriptor.

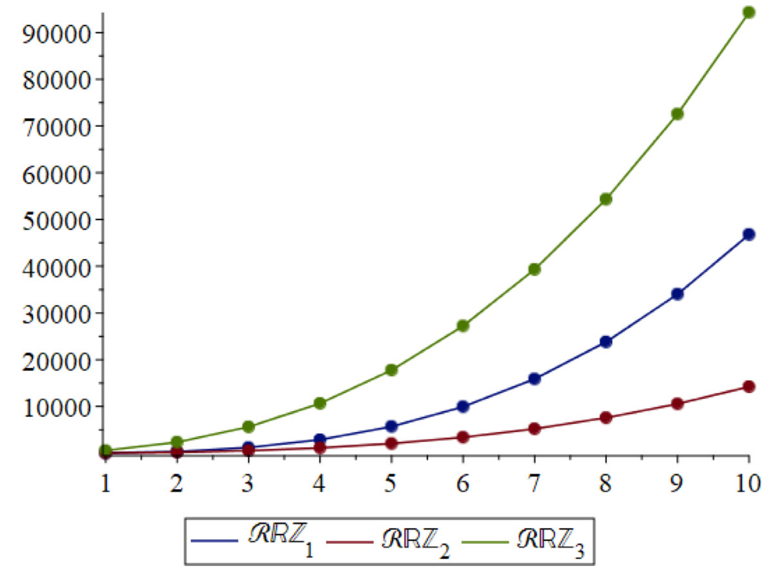

Fig. 4 Graphical analysis of reverse redefined indices for sodalite materials networks, x-axis shows the numeral values of parameters l, w, h and y-axis shows the resulted values of descriptor.

Table 1 Statistical analysis of $r\mathbb{ABC}, r\mathbb{GA}, r\mathbb{M}_1, r\mathbb{HM}$ and $r\mathbb{F}$ for sodalite materials networks.

[l,w,h]	$r\mathbb{ABC}$	$r\mathbb{GA}$	$r\mathbb{M}_1$	$r\mathbb{HM}$	$r\mathbb{F}$
[1, 1, 1]	25.456	81.254	144	574	288
[2, 2, 2]	118.79	327.76	768	2624	1344
[3, 3, 3]	280.01	883.53	2160	6714	3456
[4, 4, 4]	509.11	1892.5	4608	13408	6912
[5, 5, 5]	806.09	3498.8	8400	23270	12000
[6, 6, 6]	1171.0	5846.3	13824	36864	19008
[7, 7, 7]	1603.7	9079.1	21168	54754	28224
[8, 8, 8]	2104.3	13341.0	30720	77504	39936
[9, 9, 9]	2672.8	18776.0	42768	105678	54432
[10, 10, 10]	3309.2	25529.0	57600	139840	72000

5. Numerical and graphical representation and discussion

In the Figs. 3 and 4, we did some comparative study and by using particular values of l, w, h. For all the theorems of the main results we set some parameteric values shown in the Tables 1 and 2, like $l, w, h \in \{1, 2, \ldots, 10\}$. The figures generated from the chosen values and equations of theorem results are shown the lowest and peak point of which topological index gain. The Fig. 3 shows that the highest value gain by $r\mathbb{GA}$ and the lowest value $r\mathbb{ABC}$, while in the next Fig. 4 $r\mathbb{ReZ}_2$ and $r\mathbb{ReZ}_3$, respectively.

Table 2 Statistical analysis of reverse redefined indices for sodalite materials networks.

$[l, w, h]$	$r\mathbb{ReZ}_1$	$r\mathbb{ReZ}_2$	$r\mathbb{ReZ}_3$
[1, 1, 1]	36	36	576
[2, 2, 2]	336	188	2352
[3, 3, 3]	1188	528	5616
[4, 4, 4]	2880	1128	10656
[5, 5, 5]	5700	2060	17760
[6, 6, 6]	9936	3396	27216
[7, 7, 7]	15876	5208	39312
[8, 8, 8]	23808	7568	54336
[9, 9, 9]	34020	10548	72576
[10, 10, 10]	46800	14220	94320

6. Conclusion

This research looked that we examined the most significant structure from zeolites structures, known as the sodalite materials network, and we represented the fetched graph of this network by $\chi_{l,w,h}$, as shown in Fig. 2. This structure's movement parameters are $l, w, h \geqslant 1$. We investigate this structure in terms of various reverse-degree-based topological indices derived from simple degree-based topological descriptors. Namely we did the discussion on following topological descriptors, the general reverse Randić, second reverse Zagreb descriptor, reverse atom-bond connectivity, arithmetic descriptor, first reverse Zagreb, the reverse hyper Zagreb, the reverse forgotten, first, second and third reverse redefined Zagreb descriptors. In future, some other topological descriptors are studied and discussed for this typical enriched structure.

Declaration of Competing Interest

The authors declare that they have no known competing financial interests or personal relationships that could have appeared to influence the work reported in this paper.

References

Ajmal, Muhammad, Nazeer, Waqas, Munir, Mobeen, Kang, Shin, Kwun, Young, 2016. Some algebraic polynomials and topological indices of generalized prism and toroidal polyhex networks. Symmetry 9 (1), 5.

Ali, Ahmad, 2020. Comparative study of ve-degree and ev-degree topological descriptors for benzene ring embedded in p-type-surface in 2d network. Polycyclic Aromat. Compd., 1–10

Alshehri, Hamdan, Ahmad, Ali, Alqahtani, Yahya, Azeem, Muhammad, 2022. Vertex metric-based dimension of generalized perimantanes diamondoid structure. IEEE Access 10, 43320–43326.

Arockiaraj, Micheal, Clement, Joseph, Paul, Daniel, Balasubramanian, Krishnan, 2021. Quantitative structural descriptors of sodalite materials. J. Mol. Struct. 1223, 128766.

Aslam, Adnan, Ahmad, Safyan, Gao, Wei, 2017. On certain topological indices of boron triangular nanotubes. Zeitschrift für Naturforschung A 72 (8), 711–716.

Azeem, Muhammad, Imran, Muhammad, Nadeem, Muhammad Faisal, 2022. Sharp bounds on partition dimension of hexagonal möbius ladder. J. King Saud Univ.- Sci. 34 (2), 101779.

Barth, T.F.W., 1932. The structures of the minerals of the sodalite family. Z. Krist. Cryst. Mater. 83, 1–6.

Catlow, C.R.A., 1992. Modeling of Structure and Reactivity in Zeolites. Academic Press, London.

Dyer, A., 1988. An Introduction to Zeolite Molecular Sieves. Wiley-Interscience, Chichester.

Eddaoudi, M., Kim, J., Vodak, D., Sudik, A., Wachter, J., OKeeffe, M., Yaghi, O.M., 2002. Geometric requirements and examples of important structures in the assembly of square building blocks. Proc. Nat. Acad. Sci. 99 (8), 4900–4904.

Gao, Wei, Younas, Muhammad, Farooq, Adeel, Virk, Abaid, Nazeer, Waqas, 2018. Some reverse degree-based topological indices and polynomials of dendrimers. Mathematics 6 (10), 214.

Hameed, Shehla, Jamil, Muhammad Kamran, Waheed, Muhammad, Azeem, Muhammad, Swaray, Senesie, 2022. Two complex graph operations and their exact formulations on topological properties. Complexity 2022, 1–15.

Hassan, I., Grundy, H.D., 1984. The crystal structures of sodalite-group minerals. Acta Crystall. Section B Struct. Sci. 40 (1), 6–13.

Hong, Gang, Gu, Zhen, Javaid, Muhammad, Awais, Hafiz Muhammad, Siddiqui, Muhammad Kamran, 2020. Degree-based topological invariants of metal-organic networks. IEEE Access 8, 68288–68300.

Jaeger, F.M., 1929. On the constitution and the structure of ultramarine. Trans. Faraday Soc. 25, 320.

Javaid, Muhammad, Zafar, Hassan, Zhu, Q., Alanazi, Abdulaziz Mohammed, 2021. Improved lower bound of LFMD with applications of prism-related networks. Mathe. Probl. Eng. 2022, 1–9.

Jayanna, Gowtham Kalkere, Swamy, Narahari Narasimha, 2021. Multiplicative reverse geometric-arithmetic indices and arithmetic-geometric of silicate network. Biointerface Res. Appl. Chem. 12 (3), 4192–4199.

Jiri, C., Herman, V.B., Avelino, C., Ferdi, S., 2007. Introduction to zeolite science andpractice. Stud. Surf. Sci 2 (1), 1058–1065.

Karagiaridi, Olga, Lalonde, Marianne B., Bury, Wojciech, Sarjeant, Amy A., Farha, Omar K., Hupp, Joseph T., 2012. Opening ZIF-8: A catalytically active zeolitic imidazolate framework of sodalite topology with unsubstituted linkers. J. Am. Chem. Soc. 134 (45), 18790–18796.

Keeffe, M.O., 1991. N-dimensional diamond, sodalite and rare sphere packings. Acta Crystallogr. 47, 748–753.

Koam, Ali N.A., Ahmad, Ali, Ahmad, Yasir, 2021. Computation of reverse degree-based topological indices of hex-derived networks. AIMS Mathematics 6 (10), 11330–11345.

Koam, Ali N.A., Ahmad, Ali, Azeem, Muhammad, Khalil, Adnan, Nadeem, Muhammad Faisal, 2022. On adjacency metric dimension of some families of graph. J. Function Spaces 2022, 1–8.

Koam, Ali N.A., Ahmad, Ali, Asim, M.A., Azeem, Muhammad, 2022. Computation of vertex and edge resolvability of benzenoid tripod structure. J. King Saud Univ.- Sci., 102208

Koam, Ali N.A., Ahmad, Ali, Azeem, Muhammad, Nadeem, Muhammad Faisal, 2022. Bounds on the partition dimension of one pentagonal carbon nanocone structure. Arabian J. Chem. 15 (7), 103923.

Kulli, V.R., 2018. Reverse zagreb and reverse hyper-zagreb indices and their polynomials of rhombus silicate networks. Annals Pure Appl. Mathe. 16 (1), 47–51.

Liu, Jia-Bao, Raza, Zahid, Javaid, Muhammad, 2020. Zagreb connection numbers for cellular neural networks. Discrete Dyn. Nature Soc. 2020, 1–8.

Mufti, Zeeshan Saleem, Anjum, Rukhshanda, Abbas, Ayesha, Ali, Shahbaz, Afzal, Muhammad, Alam, Ashraful, 2022. Computation of vertex degree-based molecular descriptors of hydrocarbon structure. J. Chem. 2022, 1–15.

Munir, Mobeen, Nazeer, Waqas, Nizami, Abdul, Rafique, Shazia, Kang, Shin, 2016. M-polynomials and topological indices of titania nanotubes. Symmetry 8 (11), 117.

Munir, Mobeen, Nazeer, Waqas, Rafique, Shazia, Kang, Shin, 2016. M-polynomial and related topological indices of nanostar dendrimers. Symmetry 8 (9), 97.

Nadeem, Muhammad Faisal, Zafar, Sohail, Zahid, Zohaib, 2016. On topological properties of the line graphs of subdivision graphs of certain nanostructures. Appl. Mathe. Comput. 273, 125–130.

Nadeem, Imran, Shaker, Hani, Hussain, Muhammad, Naseem, Asim, 2019. Topological indices of para-line graphs of v-phenylenic nanostructures. Open Mathe. 17 (1), 260–266.

Nadeem, Muhammad Faisal, Azeem, Muhammad, Farman, Iqra, 2021. Comparative study of topological indices for capped and uncapped carbon nanotubes. Polycyclic Aromat. Compd., 1–18

Nadeem, Muhammad Faisal, Azeem, Muhammad, Siddiqui, Hafiz Muhammad Afzal, 2021. Comparative study of zagreb indices for capped, semi-capped, and uncapped carbon nanotubes. Polycyclic Aromat. Compd., 1–18

Nadeem, Muhammad Faisal, Imran, Muhammad, Siddiqui, Hafiz Muhammad Afzal, Azeem, Muhammad, Khalil, Adnan, Ali, Yasir, 2021. Topological aspects of metal-organic structure with the help of underlying networks. Arabian J. Chem. 14 (6), 103157.

Neeraj, S., Noy, M.L., Rao, C.N.R., Cheetham, A.K., 2002. Sodalite networks formed by metal squarates. Solid State Sci. 4 (10), 1231–1236.

Pauling, L., 1930. The structure of sodalite and helvite. Zeitschrift für Kristallographie 74, 213–225.

Poojary, Prasanna, Shenoy, Gautham B., Narahari, N., Raghavendra, A., Sooryanarayana, B., Poojary, Nandini, 2022. Reverse topological indices of some molecules in drugs used in the treatment of h1n1. Biointerface Res. Appl. Chem. 13 (1), 71.

Prabhu, S., Murugan, G., Cary, M., Arulperumjothi, M., Liu, J.-B., 2020. On certain distance and degree based topological indices of zeolite lta frameworks. Mater. Res. Express 7, 055006.

Randic, Milan, 1975. Characterization of molecular branching. J. Am. Chem. Soc. 97 (23), 6609–6615.

Refaee, Eshrag A., Ahmad, Ali, 2021. A study of hexagon star network with vertex-edge-based topological descriptors. Complexity 2021, 1–7.

Shabbir, Ayesha, Nadeem, Muhammad Faisal, Mukhtar, Safyan, Raza, Ahsan, 2020. On edge version of some degree-based topological indices of HAC5c7 [p, q] and VC5c7[p, q] nanotubes. Polycyclic Aromat. Compd., 1–17

Siddiqui, Muhammad Kamran, Imran, Muhammad, Ahmad, Ali, 2016. On zagreb indices, zagreb polynomials of some nanostar dendrimers. Appl. Mathe. Comput. 280, 132–139.

Taylor, D., 1967. The sodalite group of minerals. Contrib. Mineral. Petrol. 16, 172–188.

Torrens, Francisco, Castellano, Gloria, 2006. Fractal dimension of active-site models of zeolite catalysts. J. Nanomater. 1–9, 2006.

Torrens, F., Castellano, G., 2019. Polarizability characterization of zeolitic br awnsted acidic sites. Recent Prog. Comput. Sci. Eng 2, 555–556.

Wang, Zhen, Chaudhry, Faryal, Naseem, Maria, Asghar, Adnan, 2020. Reverse zagreb and reverse hyper-zagreb indices for crystallographic structure of molecules. J. Chem. 2020, 1–12.

Zahra, Nida, Ibrahim, Muhammad, Siddiqui, Muhammad Kamran, 2020. On topological indices for swapped networks modeled by optical transpose interconnection system. IEEE Access 8, 200091–200099.

Zhang, Jing, Siddiqui, Muhammad Kamran, Rauf, Abdul, Ishtiaq, Muhammad, 2020. On ve-degree and ev-degree based topological properties of single walled titanium dioxide nanotube. J. Cluster Sci. 32 (4), 821–832.

Zhao, Dongming, Chu, Yu-Ming, Siddiqui, Muhammad Kamran, Ali, Kashif, Nasir, Muhammad, Younas, Muhammad Tayyab, Cancan, Murat, 2021. On reverse degree based topological indices of polycyclic metal organic network. Polycyclic Aromat. Compd. 12, 1–18.